

S16. Investigation of the Microwave Carbothermic Reduction of Powdered Magnetite with the Integrated Microscopic Imaging Spectrometer

Matsubara, A., Okajima, S. (Chubu Univ.),
Takayama, S., Ida, K., Sato, M.

The microwave-heating technology accumulated through the nuclear fusion research has contributed to the field of industrial microwave processing. One of the innovations is microwave iron making¹⁾. The fundamental chemical equation for iron carbothermic reduction is $\text{Fe}_3\text{O}_4 + 2\text{C} \rightarrow 3\text{Fe} + 2\text{CO}_2$ – 317 kJ/mol. The reduction energy depends on combustion of carbon in the conventional blast furnaces. The microwave method allows to reduce the CO_2 emission by half from the level in the blast furnaces, if the electric power for the microwave is generated by carbon-free energy, such as solar, hydro and nuclear power.

A feature in the reduction process during the microwave heating is a sudden rise in material temperature from ~700 °C to ~1000 °C accompanied by light emission of atmospheric plasma²⁾. The nature of the rise in temperature has been believed to be due to the emergence of an additional channel of energy into the material through the plasma. The role of the plasma on the reduction process has been investigated by means of emission spectroscopy²⁾. Here, we present the experimentally obtained spatially-resolved spectral images of which horizontal and vertical axes are corresponding to wavelength and the slit direction of the spectrograph, respectively. The vertical extent of the image covers the boundary region of the raw material.

The employed spectroscopic system is the Integrated Microscopic Imaging System (IMIS) at NIFS. The main feature of the IMIS is integration of a microscope and an 2D-imaging spectrograph (see Fig.1). This allows us to observe emission spectrum two-dimensionally in parallel with checking the current position of the spectrum detection on the microscope image. The imaging spectrograph has a lens-slit Czerny-Turner configuration. The camera lens in that configuration minimizes aberration of astigmatism due to the collimator mirror.

The specimen was made of magnetite and graphite powders of which grain sizes were <1 μm and ca. 5 μm, respectively. The composite powder (0.619 g in mass) was shaped into a cylindrical rod of 8-mm in diameter and 10-mm in length. The specimen was set inside the quartz cell, and was heated by E-field of microwave (cw 2.450 GHz around 120 W) in the TE₁₀₃-single mode cavity. The quartz cell was evacuated by the rotary pump and refilled with helium gas before the heating. Continuous helium gas flow of 20 ml/min was used for maintaining a pressure a little higher than ambient pressure of 1 atm during the heating.

Figs. 2 and 3 show a typical set of images (visible and spectral) for during- and post-reduction period, respectively. During the reduction period (Fig. 2) the bright emission with jet appears above the surface of material. In this case iron atomic spectra are superimposed on the strong continuous spectrum. The continuous spectrum is due to the thermal radiation of the powder in the plasma. The mixture of

plasma-powder can be formed in such a way that the powder is blown into the air by CO/CO₂ gas resulting from the reduction reaction and/or by adiabatic expansion by a localized heating (likely due to a micro scale arc discharge). As shown in Fig. 3, there is no bright emission as well as continuous spectrum above the material. On the other hand, molecular band spectra of both C₂ and CO appear at the edge of the material, suggesting the rise of highly non-thermal equilibrium. This is consistent with the disappearance of the plasma-powder mixture, since the waning of the plasma-powder interaction impedes thermalization. These observations indicate the importance of plasma-powder interaction for the reduction process in microwave iron making.

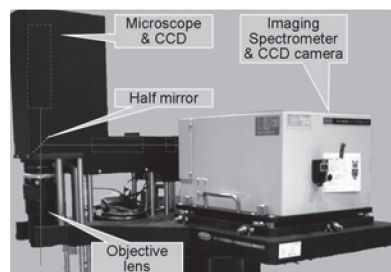


Fig. 1. Structure of the IMIS.

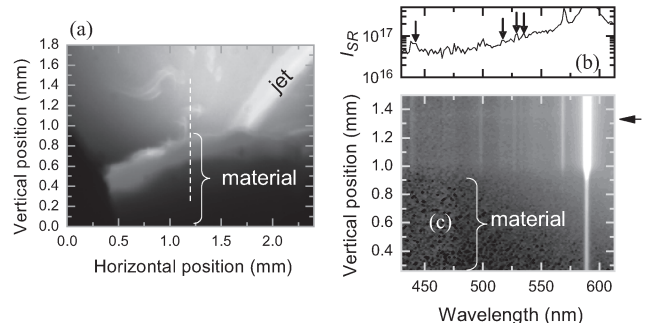


Fig. 2. The visible (a) and spectral (c) images of specimen captured at the reduction period. The dashed line in (a) shows the position of the detection of the spectral image. The emission spectrum in (b) is for the vertical position of 1.33 mm indicated by the arrow in (c). Arrows in (b) shows spectra assigned as Fe I. The strong lines at 569 nm and 590 nm are Na I.

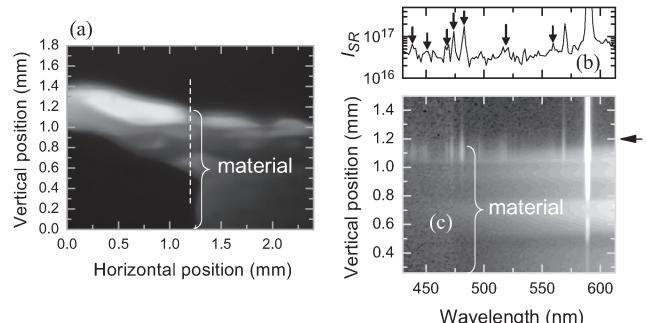


Fig. 3. The visible (a) and spectral (c) images of specimen captured at the post reduction period. Arrows in (b) shows spectra assigned as CO ($\text{B}^1\Sigma - \text{A}^1\Pi$) and C₂ ($\text{A}^3\Pi_g - \text{X}^3\Pi_u$).

1) Ishizaki K., and Nagata K.: ISIJ Intern. 46 (2006) 1403.

2) Matsubara A., et al.: PFR 3 (2008) S1085.